Drug Delivery

DOI: 10.1002/anie.201001046

Facile Two-Step Synthesis of Porous Antigen-Loaded Degradable Polyelectrolyte Microspheres**

*Marijke Dierendonck, Stefaan De Koker, Claude Cuvelier, Johan Grooten, Chris Vervaet, Jean-Paul Remon, and Bruno G. De Geest**

Without doubt, the development of vaccines constitutes one of the major breakthroughs of human medicine, allowing us to prevent numerous infectious diseases.[1] Nevertheless, for major killers such as HIV, malaria, and tuberculosis, no effective vaccine is currently available. The failure of current vaccination strategies to elicit cellular immune responses, especially CD8 cytotoxic T cells (CTLs) that can recognize and eliminate infected cells, is considered to be one of the major reasons for this failure.[2–4] Consequently, there is an urgent need to develop new vaccine formulations that can induce such CTL responses. One of the most promising approaches to achieve this goal is the encapsulation of antigens in particulate carriers with dimensions between 0.1 and 10 μm.[5] A plethora of studies has now demonstrated that such carriers can strongly enhance antigen presentation by dendritic cells (DCs), the most potent antigen presenting cells capable of priming effector T cell responses, not only quantitatively but also qualitatively. Antigen being presented by a DC as an MHC/peptide complex (MHC = major histocompatibility complex) to the T cell receptor indeed constitutes the first step in the initiation of T cell responses. Two different pathways occur for antigen presentation by MHC I and MHC II to CD8 and CD4 T-cells, respectively. MHC I presentation is responsible for the processing and presentation of cytosolic proteins, which are cleaved by the proteasome, transported to the endoplasmatic reticulum, and subsequently loaded onto MHC I molecules. By contrast, MHC II presentation occurs for endocytosed proteins, which are degraded in endolysosomal compartments, loaded onto MHC II molecules and subsequently presented at the cell surface.

[*] M. Dierendonck,[+] Dr. S. De Koker,[+] Prof. Dr. C. Vervaet, Prof. Dr. J.-P. Remon, Dr. B. G. De Geest
Laboratory of Pharmaceutical Technology
Department of Pharmaceutics, Ghent University
Harelbekestraat 72, 9000 Ghent (Belgium)
E-mail: br.degeest@ugent.be
Prof. Dr. C. Cuvelier
Department of Pathology, Ghent University
De Pintelaan 185, 9000 Ghent (Belgium)
Dr. S. De Koker,[+] Prof. Dr. J. Grooten
Laboratory of Molecular Immunology, Department of Biomedical Molecular Biology, Ghent University, Ghent (Belgium)
[+] These authors contributed equally.

[**] S.D.K. thanks Ghent University (BOF-GOA) for funding B.G.D.G. thanks the FWO-Vlaanderen for a postdoctoral scholarship.
Supporting information for this article is available on the WWW under http://dx.doi.org/10.1002/anie.201001046.

The way in which antigen is internalized by a DC, however, strongly affects how the antigen is processed and presented by a DC, and consequently also the type and strength of immune response induced. Although soluble antigens are almost exclusively presented by MHC II to CD4 T cells, particulate antigens not only are far more efficiently taken up by DCs, but are also presented by MHC I to CD8 T cells,[6] thus enabling the induction of CTL responses. Although particulate carriers have the capacity to evoke potent cellular immunity, their clinical application has been impeded largely by practical problems involving their generation, including a low antigen encapsulation efficiency, the use of chemical solvents and physical stresses that negatively affect antigen stability, and the involvement of complex and labor-intensive multistep processes to generate them.

Polymeric multilayer capsules[7–13] have emerged as promising microscopic carriers for the delivery of antigens to DCs, overcoming some of the problems described above.[14–17] These capsules are based on alternate deposition of polymers (so-called layer-by-layer technology),[18,19] either through electrostatic interaction[20–22] or hydrogen bonding,[23] onto a sacrificial template, followed by decomposition of the template, resulting in hollow capsules and allowing efficient antigen encapsulation under non-denaturing conditions. Several papers have now demonstrated the potential of these capsules to target antigens to APCs both in vitro and in vivo, resulting in strongly enhanced antigen presentation to CD4 and CD8 T cells and the induction of broad and strong immune responses.[14,16,17,24–27] The major advantage for their success is presumably threefold:[14,28] 1) They protect the antigen from degradation before reaching DCs; 2) Because of their size (1–10 μm), they are preferably targeted to DCs; and 3) Because of their soft thin shell, which is prone to the reductive conditions or endosomal proteases depending on the nature of the capsule shell, they allow the antigen to be readily processed upon internalization by DCs. Moreover, these capsules have been shown to be biocompatible and degradable, both in vitro and in vivo. Notwithstanding their excellent performance, polymeric multilayer capsules are fabricated in multiple steps, which is a rather cost-inefficient fashion involving the use of a large excess of polymer and several centrifugation steps during deposition of each single layer. Therefore, a simple and versatile strategy involving a minimum of process steps that mimics polymeric multilayer capsules would be of uttermost importance to allow this type of antigen carriers to reach the clinical stage.

Herein, we report on the synthesis of porous antigen-loaded degradable polyelectrolyte microspheres using spray drying as a simple, yet efficient, and scalable production

technique. Figure 1 shows a schematic illustration of the formation of these porous microspheres. Key in our present work is the use as a sacrificial component of calcium carbonate nanoparticles, which are directly spray-dried in combination with antigen and oppositely charged polyelectrolytes to form a polyelectrolyte framework that entraps the antigen and the calcium carbonate nanoparticles. Extraction of calcium carbonate subsequently leads to porous microspheres. We reasoned that a porous system exhibits a much higher surface to volume ratio, which, upon internalization by DCs, will enhance the access of proteases to the encapsulated antigen followed by antigen processing and initiation of the immune response.

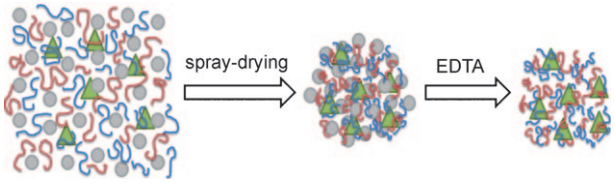

Figure 1. Schematic illustration of the encapsulation of antigen (green triangles) into porous polyelectrolyte (red and blue curves) microspheres by spray-drying a mixture of antigen, polyelectrolytes, and calcium carbonate nanoparticles ($CaCO_3^{NP}$; gray disk) followed by extraction of $CaCO_3^{NP}$ by treatment with edta.

Calcium carbonate nanoparticles ($CaCO_3^{NP}$) with an average diameter of 90 nm and a ζ-potential of 6.8 ± 0.4 mV were mixed with dextran sulfate (DS) and ovalbumin (OVA; used as model antigen in this work) under stirring. The slightly cationic surface charge of $CaCO_3^{NP}$ means that anionic DS and OVA will at least partly associate with $CaCO_3^{NP}$ through electrostatic interaction and presumably also by physical adsorption. Subsequently poly-L-arginine (P_LARG) was added dropwise to allow further electrostatic complexation between P_LARG and DS or OVA. Hollow polyelectrolyte multilayer capsules based on $CaCO_3$ microparticle templates coated with DS and P_LARG have been shown by our group to be nontoxic and degradable upon cellular uptake, both in vitro and in vivo.[29,30] In this work, the ratio of $CaCO_3$ to OVA, DS, and P_LARG was 40:1:4:5, respectively, which tends to mimic the conditions used for the encapsulation of OVA into hollow DS/P_LARG multilayer capsules templated on OVA co-precipitated $CaCO_3$ microparticles, reported in our previous work[14,15] and by others.[31] Subsequently, the mixture was spray-dried using a Buchi B290 benchtop spray-drier and collected as a dry powder comprising 80% $CaCO_3$. These particles are refered to as solid microspheres further in this paper. Porous microspheres were obtained by re-suspending the dry powder in an aqueous 0.2 M solution of ethylenediaminetetraacetic acid (edta), which is a potent complexing agent for calcium ions[32,33] and serves to extract $CaCO_3^{NP}$ from the solid microspheres.[31] The characteristics of the these spray-dried microspheres before (solid) and after (porous) $CaCO_3$ dissolution are summarized in Table 1.

The morphologies of the $CaCO_3$ nanoparticles, the solid microspheres, and the porous microspheres were visualized by scanning electron microscopy (SEM; Figure 2A).

Table 1: Overview of microsphere characteristics ($n = 3$).

	ζ-Potential	Size	OVA encapsulation
solid microspheres	-6.8 ± 0.4 mV	6.0 ± 0.4 μm	94 ± 1 %
porous microspheres	-18 ± 0.7 mV	5.8 ± 0.1 μm	86 ± 1 %

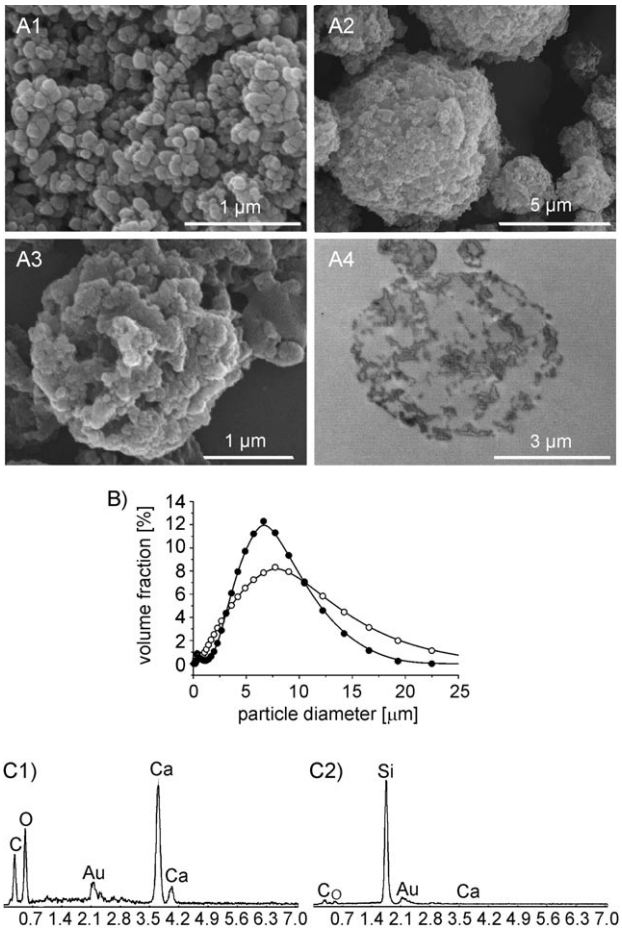

Figure 2. Scanning electron microscopy images of A1) $CaCO_3^{NP}$ (note that the aggregation is due to drying of the sample prior to SEM imaging), A2) spray-dried $CaCO_3^{NP}$/DS/OVA/P_LARG microspheres, and A3) porous DS/OVA/P_LARG microspheres after treatment with edta. A4) Transmission electron microscopy image of porous DS/OVA/P_LARG microspheres after treatment with edta. B) Size distribution of solid spray-dried $CaCO_3^{NP}$/DS/OVA/P_LARG microspheres (●) and porous DS/OVA/P_LARG microspheres obtained after treatment with edta (○). C) Energy-dispersive X-ray (EDX) spectra of C1) solid spray-dried $CaCO_3^{NP}$/DS/OVA/P_LARG microspheres and C2) porous DS/OVA/P_LARG microspheres obtained after treatment with edta.

$CaCO_3^{NP}$ exhibited a primary particle size of roughly 90 nm (Figure 2A1) and upon spray-drying are grouped into spherical clusters (Figure 2A2) with an average size of 6 μm (Figure 2B; note that some polydispersity is inherent to spray drying[34]) and a ζ-potential of −6,8 mV, as determined by laser diffraction (Figure 2A) and dynamic light scattering, respectively, upon resuspension in aqueous medium. Most

importantly, as is addressed below in more detail by confocal microscopy, the spray-dried microspheres remain stable upon resuspension in aqueous medium and do not disassemble into the initial starting components. As a control we also spray-dried a mixture of $CaCO_3^{NP}$ and OVA, and no cluster formation was observed (data not shown), indicating the requirement of the DS/P_LARG polyelectrolyte complex framework to obtain stable microspheres. Extraction of the $CaCO_3^{NP}$ by an aqueous edta solution leads to the formation of porous microspheres (Figure 2 A3,4), which have a ζ-potential of -18 mV and are most likely stabilized through a combination of electrostatic and hydrophobic interactions together with physical entanglements of the polymer and protein chains. Short-range hydrophobic forces play a major role in the formation of polyelectrolyte complexes. These originate from contact between hydrophobic parts of the polyelectrolyte chains, excluding hydration molecules.[35] The highly porous state of the microspheres is highlighted in the transmission electron microscopy of Figure 2 A4 and complete removal of the $CaCO_3^{NP}$ by treatment with edta was confirmed by energy-dispersive X-ray (EDX) analysis. The EDX spectrum shown in Figure 2 C of the solid (C1) microspheres clearly exhibits two calcium peaks, which are lacking in the EDX spectrum of the porous (C2) microspheres. Figure 2 C2 exhibits a predominant silicon peak. This silicon peak is most likely due to the porous structure of the microspheres, which allows the electron beam to reach the underlying silicon wafer on which the microspheres were deposited upon sample preparation. Laser diffraction (Figure 2 B) did not show any significant change in mean diameter of the porous microspheres compared to the solid ones, indicating that upon $CaCO_3^{NP}$ removal no substantial shrinkage or swelling of the polyelectrolyte framework occurs.

Confocal microscopy was used to visualize the microspheres in a hydrated state. For visualization purposes, green fluorescent OVA-alexa488 was mixed with native OVA in a 50:1 ratio. The confocal micrographs in Figure 3 A confirm that the microspheres remain stable in aqueous medium. When the microspheres were resuspended in 0.2 M edta, the dark shine in the transmission channel (Figure 3 A2) vanished and transparent (Figure 3 B2) "sponge-like" porous microspheres were obtained (Figure 3 B). Importantly, the green fluorescent OVA-alexa488 was retained within the polyelectrolyte framework of the porous microspheres rather than being spontaneously released into the surrounding aqueous medium.

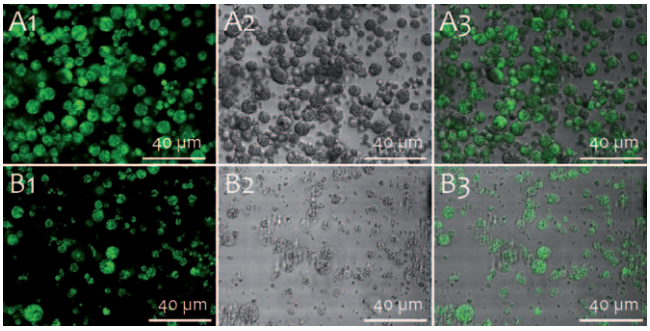

Figure 3. Confocal microscopy images of A) spray-dried solid $CaCO_3^{NP}$/DS/OVA/P_LARG microspheres and B) porous DS/OVA/P_LARG microspheres obtained after treatment with edta. The green fluorescence is due to OVA-alexa488.

Quantification of the encapsulation efficiency was determined by resuspending dry solid microspheres in phosphate-buffered saline (PBS; pH 7.4) and in an aqueous 0.2 M edta solution. Subsequently, the microspheres were centrifuged, and the OVA concentration in the supernatant was determined. An encapsulation efficiency (defined as the amount of protein that is retained within the microspheres upon resuspension relative to the amount of protein in the dry microspheres) of 94 ± 1% upon resuspension in PBS and of 85 ± 1% upon resuspension in aqueous 0.2 M edta was observed. These results show that upon resuspension in PBS only 6 ± 1% of the OVA is released from the solid microsphere whereas 15 ± 1% of the OVA is released upon extraction of the $CaCO_3^{NP}$ from the microspheres. The higher amount of released OVA from the porous microspheres relative to that from the solid microspheres is attributed to the higher surface area of the porous ones, allowing OVA that is weakly bound to the surface to be released. However, an encapsulation efficiency of 85% into the porous polyelectrolyte spheres is considerable higher than the value of approximately 50% that we reported earlier for encapsulation of OVA into hollow polyelectrolyte multilayer capsules. In that case, OVA was co-precipitated into calcium carbonate microparticles by mixing it with calcium chloride and sodium carbonate. After alternate coating of these microparticles with dextran sulfate and poly-L-arginine and subsequent dissolution of the $CaCO_3$ microparticles approximately 50% of the OVA was lost by diffusion through the polyelectrolyte membrane.

As it is our aim to use the porous polyelectrolyte microspheres as antigen carriers for vaccination purposes, it is important to assess whether these porous microspheres are able to deliver their payload to DCs. Murine DCs were differentiated from bone marrow and incubated with OVA-alexa488 loaded porous microspheres followed by confocal microscopy imaging. To discriminate whether the microspheres were internalized by DCs, we counterstained the cell nuclei blue fluorescent with Hoechst stain and the cell membrane red fluorescent with Cy5 conjugated cholera toxin B (Figure 4 A,B). As the green fluorescent microspheres, cell nuclei, and cell membrane were visible in the same confocal plane and the microspheres were clearly situated within the boundaries of the cell membrane, we could unambiguously conclude that the microspheres were effectively internalized by the DCs. The Supporting Information contains a *z*-stack of the zoomed image, which supports our conclusion. In a subsequent series of experiments to assess the intracellular localization of the porous microspheres, we counterstained with red fluorescence the cellular cytoplasm (CellTracker Red; Figure 4 C) and the intracellular acidic vesicles, such as endosomes and lysosomes (LysoTracker Red; Figure 4 D). Colocalization between green and red fluorescence, yielding a yellow/orange signal indicated by orange arrows in Figure 4 D1, shows the presence of the porous microspheres in that specific compartment. Porous

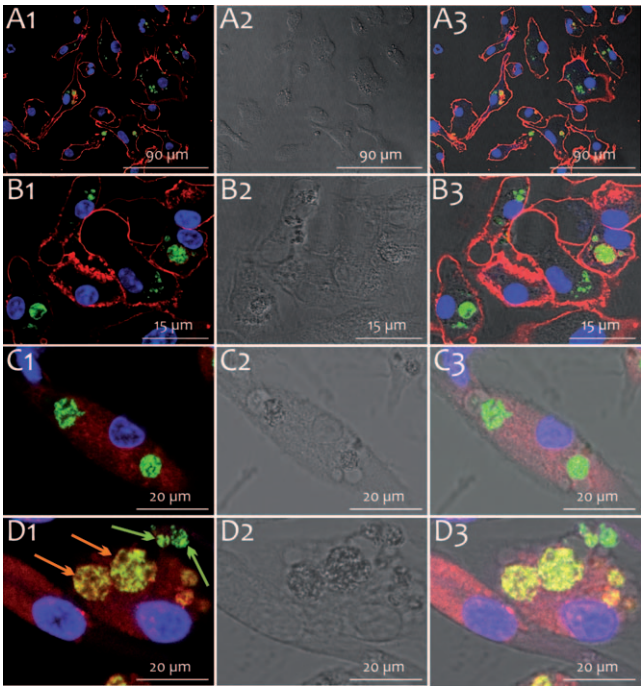

Figure 4. Confocal microscopy images of bone marrow dendritic cells incubated with green fluorescent OVA-alexa488 loaded porous microspheres. The cell nuclei in all panels were stained blue fluorescent with Hoechst stain. Panels (A) and (B), taken at different zoom levels, show images where Cy5-conjugated cholera toxin B was used to stain the cell membrane. Panels (C) show images in which CellTracker Red (red fluorescence) was used to stain the cellular cytoplasm and panels (D) show images in which LysoTracker Red (red fluorescence) was used to stain intracellular acid vesicles. In panel (D1), colocalization between red and green fluorescence (a yellow/orange signal indicates cellular uptake of the porous microspheres) is annotated with an orange arrow. Porous microspheres that are not yet taken up only exhibit a green signal and are annotated in panel (D1) with a green arrow. Panels (1) show the overlay of blue, green, and red fluorescence channels, panels (2) show the differential interference contrast (DIC) channel, and panels (3) show the overlay of blue, green, red, and DIC channels.

microspheres that do not colocalize with the endosomes only yield a green signal and are indicated in Figure 4 D1 with a green arrow. When comparing the images in Figure 4 C and D, one can unambiguously conclude that the porous microspheres are located in intracellular acidic vesicles. This result is in agreement with literature data on microparticles with similar sizes and composition.[29,36,37]

In conclusion, we have demonstrated a facile method to encapsulate antigen into porous degradable polyelectrolyte microspheres. The major advantage of this approach is the possibility to produce these microspheres on a large scale involving a minimum of process steps combined with a high encapsulation efficiency to minimize waste of expensive antigen and polyelectrolytes. The conceptual simplicity of the porous microspheres makes it possible to further tailor the microsphere surface with specific ligands with immune-potentiating properties such as oligonucleotides containing unmethylated CpG motifs.[6] Furthermore, we have demonstrated that the porous microspheres are efficiently taken up by DCs, which are the most potent antigen presenting cells. These types of microspheres could be promising vaccine delivery systems, and we are performing in vitro and in vivo DC activation and T-cell proliferation assays to elucidate the potential of the porous microspheres to efficiently target and activate the immune system. The presented approach for polyelectrolyte microsphere formation is not restricted only to antigen encapsulation/delivery but could find the same broad applications as multilayer capsules, such as enzymatic microreactors,[38,39] gene delivery,[40,41] and low molecular weight drug delivery.[42]

Experimental Section

Materials: Calcium carbonate nanoparticles ($CaCO_3^{NP}$) were obtained from Plasmachem. Dextran sulfate (DEXS; 10 kDa), poly-L-arginine (P_LARG, 100 kDa), ovalbumin (OVA; grade VII), and Hoechst 33258 were obtained from Sigma–Aldrich. OVA-alexa488, Cy5 conjugated cholera toxin B, LysoTracker Red, and CellTracker Red were obtained from Invitrogen. All water used in the experiments was of Milli-Q grade.

Synthesis of (porous) microspheres: $CaCO_3^{NP}$, DS, OVA, and P_LARG were mixed in water in a 40:4:1:5 ratio at a total solid concentration of 1 %. In detail, 200 mg $CaCO_3^{NP}$, 20 mg DS, and 5 mg OVA were dissolved in 20 mL water. Subsequently 25 mg P_LARG was dissolved in 5 mL water and added dropwise to the stirring $CaCO_3^{NP}$/DS/OVA dispersion. Spray-drying of this mixture was performed in a lab-scale Bucchi B290 spray-dryer. The mixture was fed to a two-fluid nozzle (diameter 0.7 mm) at the top of the spray-dryer. In addition, the spray-dryer operated in cocurrent air flow at 35 $m^3 h^{-1}$ with an inlet drying air temperature of 130 °C and an outlet drying air temperature of 65 °C. Owing to evaporation of the liquid, the temperature in the droplet itself is significantly lower than that in the air stream.[34]

Particle characterization: Laser diffraction was performed on a Malvern Mastersizer equipped with an RF300 objective. ζ-Potential measurements were performed on a Malvern Nanosizer ZS. Confocal microscopy images were recorded on a Leica SP5 AOBS confocal microscope. Scanning electron microscopy images and EDX-spectra were recorded on a quanta FEG FEI 200 apparatus. Samples were dried on a silicon wafer and sputtered with an ultrathin layer of palladium/gold. Transmission electron microscopy images of ultrathin microtomed sections were recorded on a JEOL 1010 electron microscope.

DC uptake assessment: Female C57BL/6 mice were purchased from Janvier and housed in a specified pathogen-free facility in micro-isolator units. Dendritic cells were generated using a modified Inaba protocol. Two- to six-month-old C57BL/6 mice were sacrificed and bone marrow was flushed from their femurs and tibias. After lysis of red blood cells with ACK lysis buffer (BioWhittaker), granulocytes and B cells were depleted using Gr-1 (Pharmingen) and B220 (Pharmingen) antibodies, respectively, along with low-toxicity rabbit complement (Cedarlane Laboratories Ltd.). Cells were seeded at a density of 2×10^5 cells mL^{-1} in 175 cm^2 Falcon tubes (Becton Dickinson) in DC medium (RPMI 1640 medium containing 5 % LPS-free FCS, 1 % penicillin/streptomycin, 1 % L-glutamine, and 50 μM β-mercaptoethanol) containing 10 ng mL^{-1} IL-4 and 10 ng mL^{-1} GM-CSF (both from Peprotech). After 2 days and again after 4 days of culture, the nonadherent cells were centrifuged, resuspended in fresh medium, and replated to the same falcons. On the 6th day, nonadherent cells were removed and fresh medium containing 10 ng mL^{-1} GM-CSF and 5 ng mL^{-1} IL-4 was added.

On day 8 of culture, nonadherent cells were harvested and seeded in Lab-Tek (Nunc, Thermo Scientific) eight-chambered cover glasses. The porous microspheres were suspended in PBS at a concentration

of corresponding of 0.5 mg mL^{-1} OVA, and 10 μL of this suspension was added to the DCs. After 2 h incubation, the cells were fixed in an aqueous 4 % formaldehyde solution overnight. Subsequently, the cells were washed three times with PBS and stained with Cy5-conjugated cholera toxin subunit B (5 μg mL^{-1})) and Hoechst 33258 (2 μg mL^{-1}). For the assessment of the intracellular localization of the porous microspheres, cells were not fixed with formaldehyde, and the cellular cytoplasm and acidic vesicles were stained by CellTracker Red (1 μg mL^{-1}) and LysoTracker Red (1 μg mL^{-1}), respectively, and visualized directly by confocal microscopy.

Received: February 19, 2010
Revised: August 27, 2010
Published online: ■■ ■■, 2010

Keywords: antigens · drug delivery · microporous materials · nanotechnology · polymers

[1] D. T. O'Hagan, N. M. Valiante, *Nat. Rev. Drug Discovery* **2003**, *2*, 727.
[2] R. Rappuoli, *Nat. Biotechnol.* **2007**, *25*, 1361.
[3] J. B. Ulmer, U. Valley, R. Rappuoli, *Nat. Biotechnol.* **2006**, *24*, 1377.
[4] S. A. Rosenberg, J. C. Yang, N. P. Restifo, *Nat. Med.* **2004**, *10*, 909.
[5] M. Singh, D. O'Hagan, *Nat. Biotechnol.* **1999**, *17*, 1075.
[6] S. Jain, W. T. Yap, D. J. Irvine, *Biomacromolecules* **2005**, *6*, 2590.
[7] F. Caruso, R. A. Caruso, H. Möhwald, *Science* **1998**, *282*, 1111.
[8] E. Donath, G. B. Sukhorukov, F. Caruso, S. A. Davis, H. Möhwald, *Angew. Chem.* **1998**, *110*, 2323; *Angew. Chem. Int. Ed.* **1998**, *37*, 2201.
[9] G. B. Sukhorukov, E. Donath, S. Davis, H. Lichtenfeld, F. Caruso, V. I. Popov, H. Möhwald, *Polym. Adv. Technol.* **1998**, *9*, 759.
[10] G. B. Sukhorukov, H. Möhwald, *Trends Biotechnol.* **2007**, *25*, 93.
[11] C. S. Peyratout, L. Dähne, *Angew. Chem.* **2004**, *116*, 3850; *Angew. Chem. Int. Ed.* **2004**, *43*, 3762.
[12] A. G. Skirtach, A. M. Javier, O. Kreft, K. Kohler, A. P. Alberola, H. Möhwald, W. J. Parak, G. B. Sukhorukov, *Angew. Chem.* **2006**, *118*, 4728; *Angew. Chem. Int. Ed.* **2006**, *45*, 4612.
[13] L. J. De Cock, S. De Koker, B. G. De Geest, J. Grooten, C. Vervaet, J. P. Remon, G. B. Sukhorukov, M. N. Antipina, *Angew. Chem.* **2010**, *122*, 7108 – 7127; *Angew. Chem. Int. Ed.* **2010**, *49*, 6954 – 6973.
[14] S. De Koker, B. G. De Geest, S. K. Singh, R. De Rycke, T. Naessens, Y. Van Kooyk, J. Demeester, S. C. De Smedt, J. Grooten, *Angew. Chem.* **2009**, *121*, 8637; *Angew. Chem. Int. Ed.* **2009**, *48*, 8485.
[15] S. De Koker, T. Naessens, B. G. De Geest, P. Bogaert, J. Demeester, S. C. De Smedt, J. Grooten, *J. Immunol.* **2010**, *184*, 203.
[16] R. De Rose, A. N. Zelikin, A. P. R. Johnston, A. Sexton, S. F. Chong, C. Cortez, W. Mulholland, F. Caruso, S. J. Kent, *Adv. Mater.* **2008**, *20*, 4698.
[17] R. Palankar, A. G. Skirtach, O. Kreft, M. Bedard, M. Garstka, K. Gould, H. Möhwald, G. B. Sukhorukov, M. Winterhalter, S. Springer, *Small* **2009**, *5*, 2168.
[18] G. Decher, *Science* **1997**, *277*, 1232.
[19] T. Boudou, Y. Crouzier, K. Ren, G. Blin, C. Picart, *Adv. Mater.* **2010**, *22*, 441.
[20] B. G. De Geest, S. De Koker, G. B. Sukhorukov, O. Kreft, W. J. Parak, A. G. Skirtach, J. Demeester, S. C. De Smedt, W. E. Hennink, *Soft Matter* **2009**, *5*, 282.
[21] B. G. De Geest, N. N. Sanders, G. B. Sukhorukov, J. Demeester, S. C. De Smedt, *Chem. Soc. Rev.* **2007**, *36*, 636.
[22] B. G. De Geest, G. B. Sukhorukov, H. Möhwald, *Expert Opin. Drug Delivery* **2009**, *6*, 613.
[23] J. F. Quinn, A. P. R. Johnston, G. K. Such, A. N. Zelikin, F. Caruso, *Chem. Soc. Rev.* **2007**, *36*, 707.
[24] A. Sexton, P. G. Whitney, S. F. Chong, A. N. Zelikin, A. P. R. Johnston, R. De Rose, A. G. Brooks, F. Caruso, S. J. Kent, *Acs Nano* **2009**, *3*, 3391.
[25] S. F. Chong, A. Sexton, R. De Rose, S. J. Kent, A. N. Zelikin, F. Caruso, *Biomaterials* **2009**, *30*, 5178.
[26] S. De Koker, T. Naessens, B. G. De Geest, P. Bogaert, J. Demeester, S. De Smedt, J. Grooten, *J. Immunol.* **2010**, *184*, 203.
[27] O. E. Selina, S. Y. Belov, N. N. Vlasova, V. I. Balysheva, A. I. Churin, A. Bartkoviak, G. B. Sukhorukov, E. A. Markvicheva, *Russ. J. Bioorg. Chem.* **2009**, *35*, 103.
[28] P. Rivera-Gil, S. De Koker, B. G. De Geest, W. J. Parak, *Nano Lett.* **2009**, *9*, 4398.
[29] B. G. De Geest, R. E. Vandenbroucke, A. M. Guenther, G. B. Sukhorukov, W. E. Hennink, N. N. Sanders, J. Demeester, S. C. De Smedt, *Adv. Mater.* **2006**, *18*, 1005.
[30] S. De Koker, B. G. De Geest, C. Cuvelier, L. Ferdinande, W. Deckers, W. E. Hennink, S. De Smedt, N. Mertens, *Adv. Funct. Mater.* **2007**, *17*, 3754.
[31] A. I. Petrov, D. V. Volodkin, G. B. Sukhorukov, *Biotechnol. Prog.* **2005**, *21*, 918.
[32] D. V. Volodkin, N. I. Larionova, G. B. Sukhorukov, *Biomacromolecules* **2004**, *5*, 1962.
[33] D. V. Volodkin, A. I. Petrov, M. Prevot, G. B. Sukhorukov, *Langmuir* **2004**, *20*, 3398.
[34] K. Masters, *Spray Drying in Practice*, SprayDryConsult International ApS, Charlottenlund, **2002**.
[35] N. A. Kotov, *Nanostruct. Mater.* **1999**, *12*, 789.
[36] O. Kreft, A. M. Javier, G. B. Sukhorukov, W. J. Parak, *J. Mater. Chem.* **2007**, *17*, 4471.
[37] A. Muñoz Javier, O. Kreft, M. Semmling, S. Kempter, A. G. Skirtach, O. T. Bruns, P. del Pino, M. F. Bedard, J. Raedler, J. Kaes, C. Plank, G. B. Sukhorukov, W. J. Parak, *Adv. Mater.* **2008**, *20*, 4281.
[38] Y. J. Wang, F. Caruso, *Adv. Mater.* **2006**, *18*, 795.
[39] Y. J. Wang, A. M. Yu, F. Caruso, *Angew. Chem.* **2005**, *117*, 2948; *Angew. Chem. Int. Ed.* **2005**, *44*, 2888.
[40] A. N. Zelikin, A. L. Becker, A. P. R. Johnston, K. L. Wark, F. Turatti, F. Caruso, *Acs Nano* **2007**, *1*, 63.
[41] A. N. Zelikin, Q. Li, F. Caruso, *Angew. Chem.* **2006**, *118*, 7907; *Angew. Chem. Int. Ed.* **2006**, *45*, 7743.
[42] Y. J. Wang, V. Bansal, A. N. Zelikin, F. Caruso, *Nano Lett.* **2008**, *8*, 1741.

Communications

Drug Delivery

M. Dierendonck, S. De Koker, C. Cuvelier, J. Grooten, C. Vervaet, J.-P. Remon, B. G. De Geest* _____ ▮▮▮▮–▮▮▮▮

Facile Two-Step Synthesis of Porous Antigen-Loaded Degradable Polyelectrolyte Microspheres

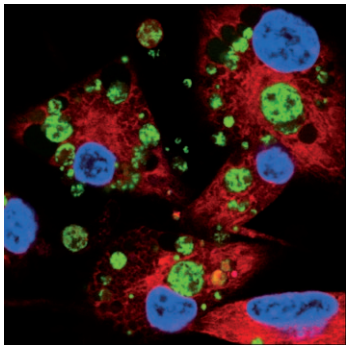

Pore medicine: Porous antigen-loaded degradable polyelectrolyte microspheres are produced in a straightforward way providing high encapsulation efficiencies and efficient internalization by antigen-presenting cells. This system could find application as multilayer capsules in gene and drug delivery and for enzymatic microreactors.